OPEN ACCESS

Case report

First-in-human endovascular treatment of hydrocephalus with a miniature biomimetic transdural shunt

Pedro Lylyk,[1] Ivan Lylyk [ID],[2] Carlos Bleise [ID],[1] Esteban Scrivano,[1]
Pedro Nicolas Lylyk,[1] Brandon Beneduce,[3] Carl B Heilman,[4] Adel M Malek [ID] [4]

Linked

► http://dx.doi.org/10.1136/neurintsurg-2021-018517

Check for updates

SUMMARY
Surgical ventriculoperitoneal shunting remains standard treatment for communicating hydrocephalus, despite persistently elevated infection and revision rates. A novel minimally invasive endovascular cerebrospinal fluid (CSF) shunt was developed to mimic the function of the arachnoid granulation which passively filters CSF from the central nervous system back into the intracranial venous sinus network. The endovascular shunt is deployed via a femoral transvenous approach across the dura mater into the cerebellopontine angle cistern. An octogenarian with intractable hydrocephalus following subarachnoid hemorrhage underwent successful endovascular shunting, resulting in swift intracranial pressure reduction from 38 to <20 cmH$_2$O (<90 min) and resolution of ventriculomegaly. This first successful development of a percutaneous transluminal venous access to the central nervous system offers a new pathway for non-invasive treatment of hydrocephalus and the potential for intervention against neurological disorders.

BACKGROUND
Communicating hydrocephalus results from an imbalance between cerebrospinal fluid (CSF) production and its resorption, leading to increased intracranial pressure and ventricular dilatation. Current standard treatment of hydrocephalus remains ventriculoperitoneal (VP) shunt surgery first introduced over 60 years ago, requiring multiple scalp, neck, and abdominal incisions, a burr hole, and catheter traversing cortex and white matter. The hydrostatic column pressure when the patient stands upright makes VP shunts prone to a siphon effect, leading to CSF overdrainage and resulting in subdural fluid or blood collections. Despite its maturity, the VP shunt has remained largely unchanged except for development of externally adjustable valves and modifications to mitigate siphoning. These incremental developments and the introduction of antibiotic-impregnated tubing have not eliminated a risk of surgical infection of around 10% and high overall VP shunt failure rates, estimated to be between 21% and 42% by the first year following placement.[1–3] A recent, National Institutes of Health-sponsored symposium noted that first-time shunts fail within 2 years at a rate of over 40%.[4]

The shortcomings of VP shunts served as impetus to seek a less invasive alternative approach for patients with communicating hydrocephalus. A biomimetic strategy inspired an approach to replicating the function of the arachnoid granulation which passively transports CSF from the subarachnoid space to the venous sinuses with a valved micro-implant (figure 1A and B) to be positioned straddling the dura mater and enable CSF flow from a brain cistern to an adjacent draining vein.[5]

Communicating hydrocephalus occurs in 6–67%[6] of patients with aneurysmal subarachnoid hemorrhage, initially requiring surgical placement of an external ventricular drain (EVD) into the non-dominant frontal horn to simultaneously drain CSF and measure intracranial pressure (ICP). At 1–3 weeks of treatment 9–36% of patients with aneurysmal subarachnoid hemorrhage are unable to wean off EVD, becoming shunt dependent and requiring VP shunt surgery,[7 8] often performed through the contralateral dominant hemisphere.[9] This patient population was deemed likely to benefit from endovascular shunting, with the concomitant ability to evaluate function through the existing EVD prior to its removal. We describe here our experience with first patient treatment using this new approach.

DEVICE DESIGN AND DEPLOYMENT
A novel minimally invasive endovascular CSF shunt was developed for delivery through a retrograde percutaneous transvenous approach from the femoral to the jugular vein (figure 1A and B). The eShunt System (CereVasc, Inc, Auburndale, Massachusetts, USA) is a miniature 3 cm long (figure 1C and D) intracranially implantable valved endovascular CSF shunt designed for transdural deployment at the inferior petrosal sinus (IPS) to establish a CSF pathway from the cerebellopontine angle (CPA) cistern to the IPS,[5] replicating arachnoid granulation function by restoring natural CSF reabsorption into the venous system.

The fixed nature of the IPS, being encased within the bony inferior petrosal sulcus and its cistern-facing dural wall make it an ideal site for accurate catheter navigation and transdural puncture (figure 1A). A proprietary two-step delivery system was designed employing initial deployment of a temporary exchange-length anchor/flat wire into the cavernous sinus/IPS junction to act as a low-profile rail for subsequent advancement
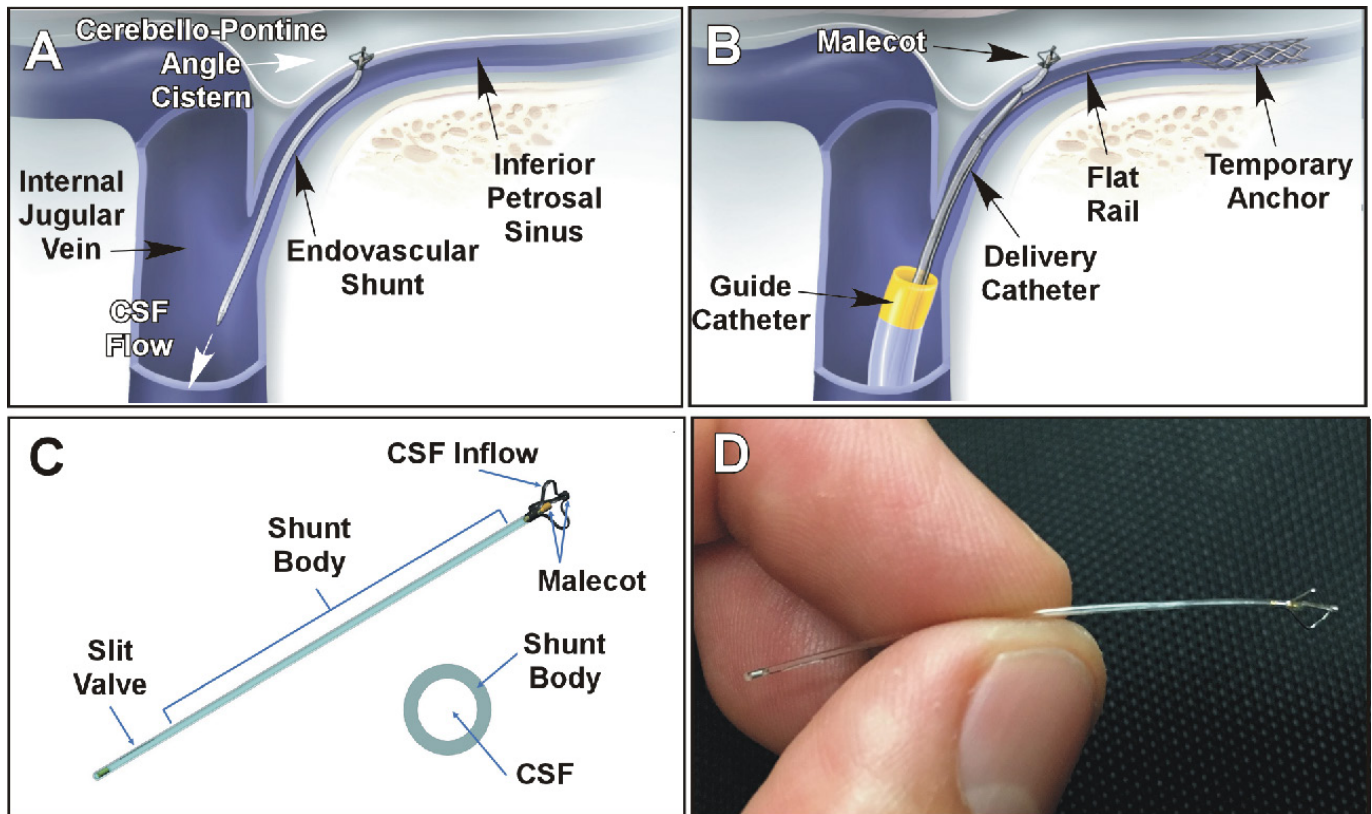
BMJ

SNIS

Figure 1 (A) An endovascular shunt in its deployed position with its tip malecot in the cerebellopontine angle cistern, draining into the internal jugular vein. (B) Endovascular technique for transdural controlled penetration using conventional venous catheterization. (C) eShunt biomimetic design with a one-way slit valve. (D) eShunt implant in close view. CSF, cerebrospinal fluid.

of the eShunt-containing delivery catheter (figure 1B). Preoperative high-resolution T1-weighted gadolinium-enhanced MRI (figure 2A) is used to segment bilateral IPS and adjacent arterial vasculature, enabling virtual simulation of the transdural trajectory and selection of the deployment site; the latter is then highlighted on the intraprocedural cone-beam CT venographic reconstruction, and the site transferred to the 3D-roadmapping guidance. This workflow enables consistent identification of the target site for deployment with fluoroscopy under various working views and magnification (figure 2A–C).

Once the delivery catheter reaches the target implantation site within the IPS, a needle on the distal tip is unsheathed and the system advanced under 3D-roadmapping guidance to slowly penetrate the taut dural wall of the IPS (figure 2D), enabling access to the adjacent CPA cistern, and controlled deployment of the endovascular shunt (figure 2E). The eShunt implant is proximally ensconced by a nitinol shroud enabling depth adjustment until final release by the operator (figure 2F). The implant's differential pressure slit valve resides within the internal jugular vein and regulates CSF flow in a pressure-driven manner proportional to the positive pressure gradient between ICP and venous blood pressure. The pressure gradient between ICP and venous pressure is estimated at 3–5 mm Hg in healthy patients and rises significantly in patients with untreated hydrocephalus.[10 11] The valve prevents blood reflux into the cistern during certain transient physiological conditions (eg, coughing, straining, sneezing) which can cause transient (<2 s) venous blood pressure spikes,[12–14] although research indicates dynamic coupling between ICP and local venous pressure with a constant favorable transdural positive pressure gradient. The implant is designed to drain 10 mL/h at a pressure gradient of ≤8 mm Hg. A sponsor-initiated (CereVasc Inc., Auburndale, Massachusetts, USA) and supported, prospective, single-center, open-label, single-arm pilot study was initiated (ClinicalTrials.Gov NCT04758611) to evaluate communicating hydrocephalus treatment using eShunt. The study was approved by an ethics committee (Stamboulian CEI S.A.), the Argentinian regulatory authority (ANMAT), and the local institutional review board.

CASE PRESENTATION

An octogenarian patient presented with subarachnoid haemorrhage (Hunt/Hess grade III; Fisher IV) from a ruptured middle cerebral aneurysm, which was secured using coils in the acute phase; an EVD was placed to treat acute communicating hydrocephalus.

INVESTIGATIONS

After most of the blood cleared from the CSF, an EVD clamp test was performed and not tolerated on day 9 as ICP increased to 44 cmH2O necessitating reopening of the drain outlet and confirming shunt dependence. Analysis of the patient's CT and gadolinium-enhanced MRI studies showed that the patient's right IPS was suitable for eShunt implant (figure 2A and B). Specifically, the IPS diameter at the target implant site above the jugular tubercle measured 3.5 mm, sufficient to accommodate the delivery catheter (figure 2A). CPA depth from target implant site to the brainstem was 6.2 mm with no vertebrobasilar arteries or cranial nerves within 5 mm, and without petrous bone obstruction (figure 2B) along the path of transdural entry to the CPA cistern (figure 2C).[5]
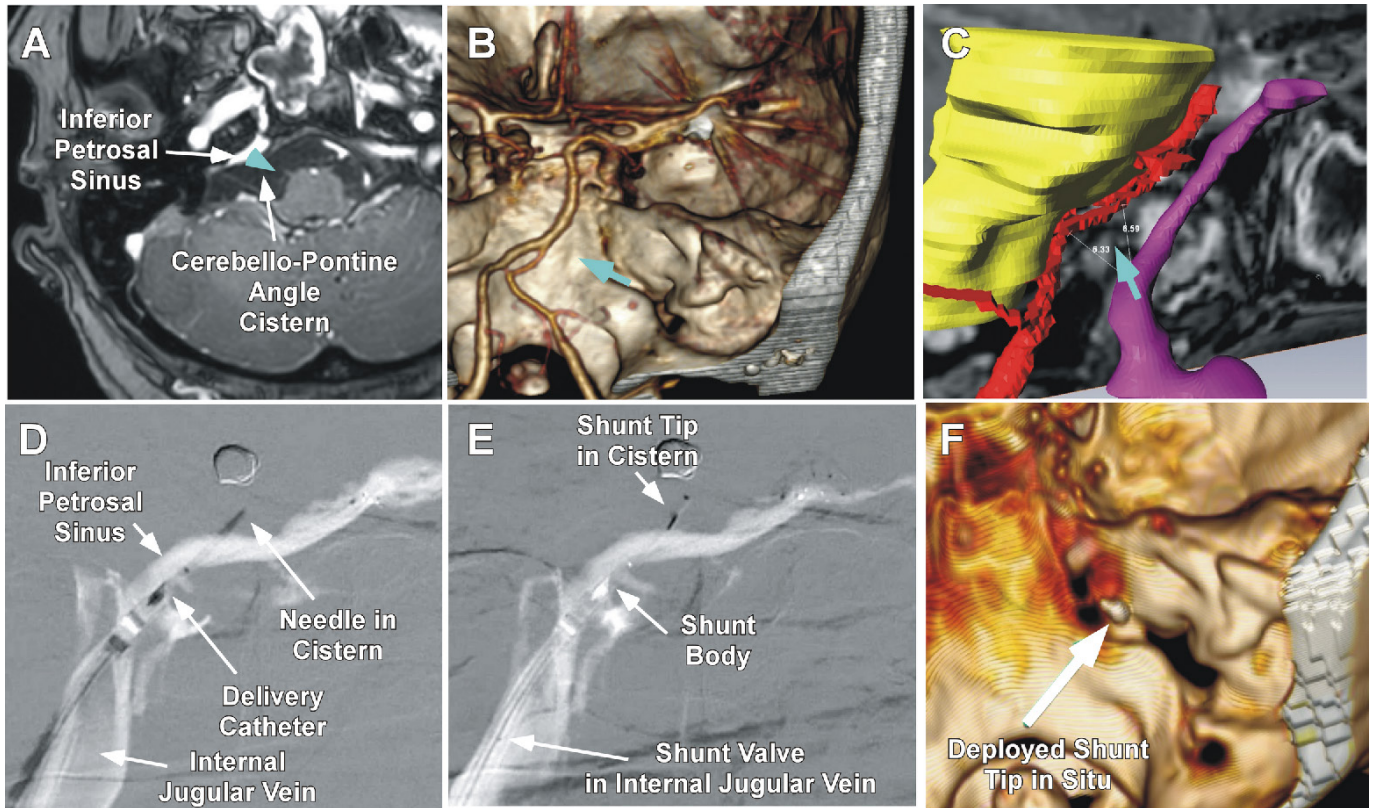
Figure 2 (A) T1-Weighted axial gadolinium-enhanced MRI scan highlights the inferior petrosal sinus (IPS) and adjacent cerebellopontine angle (CPA) cistern (arrow showing intended transdural device placement). (B) Three-dimensional rendering of computed tomographic angiography with arrow highlighting intended transdural trajectory for deployment. (C) Segmentation from T1-gadolinium- enhanced MRI scan highlights the IPS (purple), vertebral and posterior inferior cerebellar artery (red) and their >6 mm distance away from the intended trajectory (arrow) for transdural egress of eShunt. (D) Intraprocedural IPS roadmap showing successful dural penetration with delivery catheter needle into the CPA cistern. (E) Successful deployment of the eShunt with its tip in the CPA cistern, its body in the IPS, and its valved tip draining into the internal jugular vein. (F) Postprocedural reconstruction of computed tomographic acquisition confirming stable position of eShunt malecot tip at intended target site.

DIFFERENTIAL DIAGNOSIS
None.

TREATMENT
Following induction of general anesthesia, percutaneous femoral venous access was obtained, and an IV heparin bolus (50 IU/kg) administered. A guide catheter was advanced retrograde in the vena cava, past the right atrium into the right internal jugular vein and into the ostium of the IPS. A microcatheter was navigated into the distal right IPS enabling a contrast injection and three-dimensional cone-beam CT acquisition highlighting IPS anatomy. The obtained 3D volume was used to select the target implantation site, and this was exported as background for 3D-roadmapping live fluoroscopy. The distal anchor/flat rail was then deployed into the distal IPS enabling careful advancement of the shunt delivery catheter to the IPS deployment target site thanks to 3D image overlay on real-time 2D fluoroscopy (figure 2D and E).

Immediately prior to transdural access, protamine (10 mg) was administered to reverse anticoagulation. An IPS venous roadmap was obtained, and the needle unsheathed and used to advance through the dural wall of the IPS in a controlled fashion, thus gaining transluminal access to the CSF cistern (figure 2D). The eShunt device contained within the needle lumen was successfully delivered into the CPA cistern under fluoroscopy (figure 2E). The delivery catheter was then withdrawn, and the anchor subsequently retrieved followed by the guide catheter

and venous sheath removal with gentle manual compression (figure 2F). Total time from venous access to closure was 125 min; total device-specific procedure time was 50 min.

OUTCOME AND FOLLOW-UP
The patient's EVD was closed prior to the procedure as with routine VP shunt surgery and ICP measured 38 cmH$_2$O immediately prior to implant deployment. Following implant deployment, ICP began to decrease immediately, reaching normal levels (<20 cmH$_2$O) within 90 min postprocedure (figure 3A). We continued to measure the patient's ICP for 39 hours after the procedure, at which time the ICP stabilized at approximately 13.5 cmH$_2$O and the EVD was removed. Three transient ICP increases occurred postprocedure (figure 3A, inset), which coincided with nursing care events and a change of the central IV line necessitating Trendelenburg position. These spikes resolved without intervention with the EVD remaining closed and without associated neurological change.

Preprocedure CT scans (figure 3B, left) showed evidence of ventriculomegaly, consistent with the hydrocephalus diagnosis. Immediate post-deployment cone-beam CT scanning in the neuroangiography suite showed no contrast extravasation into the CSF cistern (figure 3B, centre). CT scans taken at 3 and 44 hours postprocedure demonstrated progressive improvement in ventricular size, consistent with declining ICP into the normal range (figure 3B, right) without blood near the visualized implant (figure 3B lower panel, centre) or signs of overdrainage/subdural
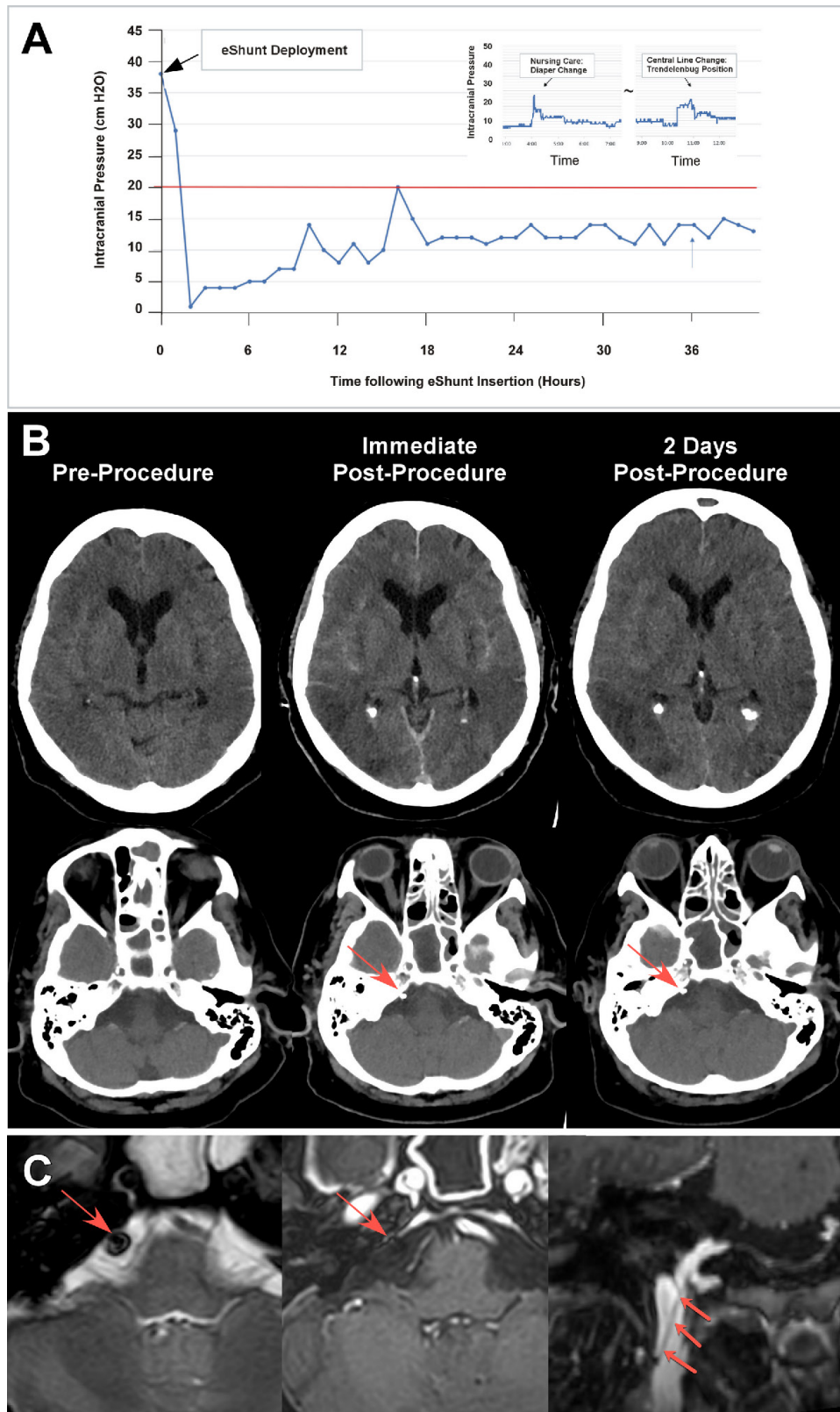
Figure 3 (A) Intracranial pressure measured through external ventricular drain following eShunt placement shows a rapid and sustained normalization; insets show transient intracranial pressure spikes coinciding with activity/postural change with return to baseline. (B) Computed tomographic scan before (left), 3 hours after eShunt procedure (contrast enhancing, centre), and at 2 days (right) show resolution of third ventricular enlargement following procedure (top panel). Corresponding cuts at the level of the eShunt insertion in to the cerebellopontine angle (CPA) cistern show no evidence of blood or extravasation at/near the malecot tip of the eShunt (arrow, bottom panel). (C) Follow-up heme-sensitive gradient echo at the level of the eShunt insertion (left) in the CPA cistern show artefactual metal blooming from the malecot (arrow) but no adjacent blood. MRI-T1-dadolinium-enhanced in axial and oblique views reveal the malecot metallic signal void adjacent to the enhancing inferior petrosal sinus (IPS; arrow, middle) as well as the body of the eShunt within the IPS and internal jugular vein (arrows, right).

fluid. MRI taken 4 days prior to the procedure confirmed ventriculomegaly, showing enlargement of the frontal and lateral horns and the third ventricle. MRI 6 days postprocedure showed a reduction in size of the frontal and lateral horns and third ventricle. No blood was visible on MRI near the deployment area on gradient echo sequence (figure 3C, left) and the implant was visualized with its malecot in the CPA cistern and valved tip in the venous system (figure 3C, right), without image distortion and minimal artifact on T1-weighted MRI (figure 3C, centre and right). Normal venous blood flow was visible through the IPS and internal jugular vein around the implant. No device or procedure-related adverse events were observed.

DISCUSSION

We describe the first endovascular treatment of communicating hydrocephalus using a novel miniature biomimetic CSF shunt, and the first successful percutaneous transluminal endovascular access to the central nervous system using a catheter-based approach. This capability offers potential for direct infusion of biopharmaceutical agents including anti-sense oligonucleotides, gene therapy, and intrathecal chemotherapy that can be hindered by inadequate CSF circulation from lumbar puncture approaches.

In addition, this case illustrates the successful resolution of elevated ICP in the acute period thanks to shunting excess CSF into the venous system. Other investigators have previously reported successful results by shunting CSF from the ventricles into the intracranial venous system via the transverse sinus, sagittal sinus, or internal jugular vein[15 16]; however, all involved an invasive surgical procedure using conventional CSF shunt tubing and componentry and requiring a burr hole and brain tissue penetration. We believe the more natural approach of mimicking the arachnoid granulations by shunting CSF to the adjacent venous system may simplify valve requirements by re-stablizing physiologic venous pressure regulation of ICP that has been disrupted in patients with communicating hydrocephalus. Thus, the simple differential pressure valve design of the endovascular shunt will increase or decrease CSF output according to the patient's own pressure gradient across the dura, as is believed to occur via arachnoid granulations. Although we have no direct flow measurement through the implant, its function is confirmed by the rapid reduction of ICP postprocedure. Furthermore, the lack of venous blood reflux in the CSF, despite several documented incidents of post-deployment transient venous pressure and ICP spikes such as during Trendelenburg positioning, supports proper functionality of the eShunt one-way valve.

The presented eShunt approach requires careful preplanning in order to avoid arteries and veins in the subarachnoid space adjacent to the dural penetration site. A thorough preprocedural planning protocol has been developed designed to avoid vascular injury during dural penetration that could result in subarachnoid or subdural hemorrhage. Reversal of anticoagulation prior to deployment could predispose to venous thrombosis of the IPS. We also do not yet know how long-term patency rates of the eShunt will compare with conventional VP shunts as it may be prone to clogging by protein or adjacent arachnoid tissue. The smaller inner diameter of the eShunt results in a substantially higher flow velocity and shorter CSF dwell time than in a VP shunt, and the absence of a mechanical valve and chamber may also help to decrease fluid stagnation and occlusion, but longer-term data are needed to answer these important questions. In the case of shunt failure or infection, multiple in vitro and cadaveric experiments have confirmed that the eShunt can be removed using a conventional foreign body retrieval device from a transvenous approach with spontaneous dural closure.

The current report represents the first account of a patient with communicating hydrocephalus being treated using an endovascular shunt system. This novel percutaneous approach might have the potential to offer patients with shunt-dependent communicating hydrocephalus a less invasive path to treatment.

LEARNING POINTS/TAKE HOME MESSAGES

► A percutaneous minimally invasive endovascular transdural access to the cerebellopontine angle cistern has been successfully achieved.
► A biomimetic cerebrospinal fluid endovascular shunt was successfully delivered via the inferior petrosal sinus to the cistern using 3D-roadmapping guidance.
► Endovascular delivery of the shunt resulted in rapid and sustained decrease in intracranial pressure consistent with cerebrospinal fluid diversion.
► This first-in-human result suggests the potential for a novel less invasive endovascular treatment of communicating hydrocephalus.
► The described percutaneous transdural access route is the first to enable endovascular access to the central nervous system for delivery of a therapeutic device or biopharmaceutical agent.

ORCID iDs
Ivan Lylyk http://orcid.org/0000-0002-6048-4225
Carlos Bleise http://orcid.org/0000-0003-2292-3263
Adel M Malek http://orcid.org/0000-0002-0642-7609

REFERENCES

1 Kofoed Månsson P, Johansson S, Ziebell M, et al. Forty years of shunt surgery at Rigshospitalet, Denmark: a retrospective study comparing past and present rates and causes of revision and infection. *BMJ Open* 2017;7:e013389.
2 Merkler AE, Ch'ang J, Parker WE, et al. The rate of complications after ventriculoperitoneal shunt surgery. *World Neurosurg* 2017;98:654–8.
3 Reddy GK, Bollam P, Shi R, et al. Management of adult hydrocephalus with ventriculoperitoneal shunts: long-term single-institution experience. *Neurosurgery* 2011;69:774–81.

4   McAllister JP, Williams MA, Walker ML, *et al*. An update on research priorities in hydrocephalus: overview of the third National Institutes of Health-sponsored symposium "Opportunities for hydrocephalus research: pathways to better outcomes". *J Neurosurg* 2015;123:1427–38.

5   Heilman CB, Basil GW, Beneduce BM, *et al*. Anatomical characterization of the inferior petrosal sinus and adjacent cerebellopontine angle cistern for development of an endovascular transdural cerebrospinal fluid shunt. *J Neurointerv Surg* 2019;11:598–602.

6   Rincon F, Gordon E, Starke RM, *et al*. Predictors of long-term shunt-dependent hydrocephalus after aneurysmal subarachnoid hemorrhage. Clinical article. *J Neurosurg* 2010;113:774–80.

7   Chen S, Luo J, Reis C, *et al*. Hydrocephalus after subarachnoid hemorrhage: pathophysiology, diagnosis, and treatment. *Biomed Res Int* 2017;2017:1–8.

8   Xie Z, Hu X, Zan X, *et al*. Predictors of shunt-dependent hydrocephalus after aneurysmal subarachnoid hemorrhage? A systematic review and meta-analysis. *World Neurosurg* 2017;106:844–60.

9   Paisan GM, Ding D, Starke RM, *et al*. Shunt-dependent hydrocephalus after aneurysmal subarachnoid hemorrhage: predictors and long-term functional outcomes. *Neurosurgery* 2018;83:393–402.

10 Glimcher SA, Holman DW, Lubow M, *et al*. Ex vivo model of cerebrospinal fluid outflow across human arachnoid granulations. *Invest Ophthalmol Vis Sci* 2008;49:4721–8.

11 Grzybowski DM, Holman DW, Katz SE, *et al*. In vitro model of cerebrospinal fluid outflow through human arachnoid granulations. *Invest Ophthalmol Vis Sci* 2006;47:3664–72.

12 Fisher J, Vaghaiwalla F, Tsitlik J, *et al*. Determinants and clinical significance of jugular venous valve competence. *Circulation* 1982;65:188–96.

13 Little WC, Reeves RC, Coughlan C, *et al*. Effect of cough on coronary perfusion pressure: does coughing help clear the coronary arteries of angiographic contrast medium? *Circulation* 1982;65:604–10.

14 Williams B. Cerebrospinal fluid pressure changes in response to coughing. *Brain* 1976;99:331–46.

15 El-Shafei IL, El-Shafei HI. The retrograde ventriculovenous shunts: the El-Shafei retrograde ventriculojugular and ventriculosinus shunts. *Pediatr Neurosurg* 2010;46:160–71.

16 Børgesen SE, Pieri A, Cappelen J, *et al*. Shunting to the cranial venous sinus using the SinuShunt. *Childs Nerv Syst* 2004;20:397–404.